Short Term Scientific Mission Report

Sheng Wang, 16-02-2016

COST Action: ES1309

STSM title: Innovative Optical Tools for Proximal Sensing of Ecophysiological Processes

Reference number: COST-STSM-ES1309-170116-070147

STSM type: Regular (from Denmark to Spain)

Applicant: Sheng Wang (swan@env.dtu.dk), A PhD student from Department of Environmental Engineering, Technical University of Denmark (DTU), Copenhagen, Denmark

Period: from 2016-01-17 to 2016-01-23

Host: Dr. Pablo Zarco-Tejada (pablo.zarco@csic.es)

Location: Laboratory for Research Methods in Quantitative Remote Sensing (QuantaLab), Institute for Sustainable Agriculture (IAS), Spanish National Research Council (CSIC), Cordoba, Spain

Introduction:

This document reports the main scientific outcome of this short term scientific mission (STSM) undertaken by me, Sheng Wang to the QuantaLab, IAS, CSIC, Cordoba, Spain during the period from 2016-01-17 to 2016-01-23. The purposes of this mission, as stated in the proposal of the STSM, are described below. Then, the work carried out and main results obtained during this period have been summarized. Finally, this report outlines future collaborations and foreseen publication.

Purpose of the STSM:

The main short-term purpose of this STSM is to receive the state of the art training in optical sampling protocols for radiometric calibration of a multispectral camera. This will speed up my research by directly learning well established calibration protocols from Quantalab enabling me to focus on making new advances in UAV-remtoe sensing research. I take a multispectral camera Tetra Mini-MCA6 from DTU-Environment to QuantaLab-IAS-CSIC for absolutely radiometric calibration, learn the protocols of radiometric calibration of a multispectral camera, assess the performance of the radiometric calibrated camera in the field, write a report on the protocol of camera radiometric calibration, and share the protocol with colleagues and use it for the Unmanned Aerial Vehicle (UAV) project at DTU, Denmark.

For the long-term, this STSM will promote the progress of my PhD project, which focuses on hyperspatial (1 meter resolution lever) mapping of energy, water and carbon dynamics with UAVs over eddy covariance flux towers, e.g. Risø in Denmark. This STSM will also promote the UAV-based remote sensing applications in Denmark. The UAV-based remote sensing is a promising technique for hyper-resolution land surface characterization, monitoring and modeling; to fill the scale discrepancy between in-situ observations (e.g. eddy covariance flux observations) and coarse resolution satellite-based remote sensing data (e.g. MODIS); to provide rich high-spatial resolution spectral data to explore the optical–biophysical relationships of vegetation.

Description of the work carried out during the STSM:

1. Visit the QuantaLab-IAS-CSIC and discuss the current progress of UAV-based remote sensing with the technicians and PhD students.
2. Learn the protocol of radiometric calibration (gain correction method) for the multi-spectral camera.
3. Use the integrating sphere to radiometrically calibrate the Tetra Mini-MCA6 camera.
4. Get the gain for each band of the camera and conduct an application to measure the radiance of typical objectives.

Description of the main results obtained:

With guidance of the technician Alberto Hornero Luque and David Notario Rosingana, the Tetra Mini-MCA6 was radiometrically calibrated at the QuantaLab-IAS-CSIC. Here, the methodology, calibration results and an application are described.

1. Methodology:

In QuantaLab-IAS-CSIC, one of most popular radiometric calibration model, the linear model as Eq. 1 (Ferrero et al., 2006; Shimano et al., 2007), was employed for radiometric calibration of the multispectral camera.

$$L = c1 \times DN + c0 \qquad \text{Eq. (1)}$$

Where L denotes the spectral radiance [W s m^{-2} sr^{-1} μm^{-1}], c1 is the gain [W s m^{-2} sr^{-1} μm^{-1}], c0 is an offset [W s m^{-2} sr^{-1} μm^{-1}], and DN denotes the digital number of the image [no unit].

L stands for the spectral radiance of the illumination from the integrating sphere. The integrating sphere is an optical instrument consisting of a hollow spherical cavity with its interior covered with a highly reflecting Bariumsulfate ($BaSO_4$). This ensures multiple diffuse reflections inside the sphere and that a uniform and homogeneous illumination will be present in the radiance port of the sphere. The integrating sphere at the QuantaLab (CSTM-USS-2000C Uniform Source System, LabSphere, NH, USA) has four tungsten lamps and corresponds to four levels of illumination (12.5, 25, 37.5 and 50 mW/cm^2-sr-μm). It was calibrated at Labsphere, Inc., Optical Calibration Laboratory.

The offset c0 is mostly related to the dark current. The dark current is due to the fact that the camera charge-coupled device (CCD) lines produce a signal even without any incoming light (Graham et al., 2004). The dark current depends on the temperature, integration time and position of pixels. The dark current could be eliminated by measuring and averaging the offset for each pixel. Thus, we took the image without any incoming light as the dark current (DN_{dark}). The image taking with light will be subtracted the dark current (DN- DN_{dark}) and then the gain (c1) could be obtained by L divided by (DN- DN_{dark}), as Eq. (2) shows:

$$c1 = \frac{L}{DN - DN_{dark}} \quad \text{Eq. (2)}$$

The coefficient c1 depends on the integration time t. It could be described as a function of t as following:

$$c1 = f(t) \quad \text{Eq. (3)}$$

With different illumination and integration times, an experiment to get the gain was set up as shown in Figure 1. The Tetra Mini-MCA6 camera was placed in front of the integrating sphere radiance port. The sphere is designed with a radiance port large enough to overfill the camera's field of view (FOV). The camera took images with different illumination conditions and integration time. One laptop (the above one in the Figure 1) was used to control the radiance of illumination from the integrating sphere. The laptop below (see Figure 1) was connected to the camera and changes its integration time. By this experiment, we can measure DN from the camera with different L. Then, the gain (c1) could be calculated. Finally, a power function was employed to fit the relationship between the gain (c1) and the integration time (t) for different spectral bands. In the application, DN from the camera images could be easily transformed to the radiance by the gain, which is determined by the integration time.

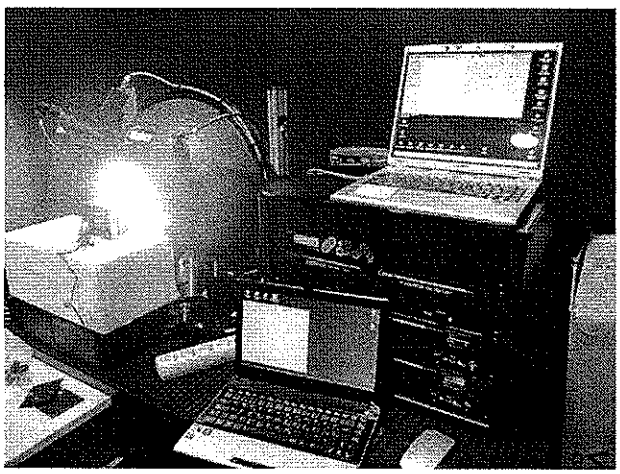

Figure 1. The setup of the experiment for measuring gain for each band of the Mini-MCA6 camera

2. Results:

The measured DN values with different integration time and illumination radiance values are summarized in the Table 1. Because with longer integration time the CCD of the camera is exposed to the illumination for a longer time, the DN values of the camera get saturated. Thus, only low illumination conditions were set with long integration time of the camera. For instance, with an integration time 4ms, the camera was only employed to take images with 0.5 and 1 illumination conditions. After these measurements were finished, by the Equation 2, we can convert these measured DNs with illumination radiance to get the gain for each integration time.

Table 1. The measurement of DN for six bands with different integration time (IT: 1-4 ms) and illumination intensities (0.5-5)

Band No.	**3**	**2**	**4**	**6**	**5**	**1**
IT 4ms	**530**	**470**	**570**	**710**	**670**	**800**
0.5	249.878	93.811	371.714	613.222	648.254	578.201
1	495.308	256.145	737.313	-	-	-
IT 3ms	**530**	**470**	**570**	**710**	**670**	**800**
0.5	175.075	62.098	262.805	432.332	458.184	406.431
1	344.905	173.819	514.021	846.736	901.917	807.951
2	-	-	-	-	-	-
IT 2ms	**530**	**470**	**570**	**710**	**670**	**800**
0.5	110.838	40.411	162.178	265.158	278.814	243.916
1	214.222	108.651	317.454	524.367	559.04	490.829
2	424.072	162.829	632.212	-	-	-
3	628.537	242.98	931.856	-	-	-
IT 1ms	**530**	**470**	**570**	**710**	**670**	**800**
0.5	54.453	27.231	81.248	131.182	129.9	115.19
1	106.004	52.866	157.759	256.567	264.228	230.729
2	206.116	105.694	309.442	503.814	531.517	467.714
3	306.749	115.685	459.719	743.845	792.773	697.054
4	405.89	156.456	606.857	-	-	-
DC	**530**	**470**	**570**	**710**	**670**	**800**
	9.408	16.002	8.882	11.449	16.001	11.194

After the gains were calculated, the relationship between the gains and the integration time for each spectral band were derived as shown in the Figure 2. Based on these power functions, users of the camera can easily get the gain to convert the DN from the camera images to the radiance. At the same time, by changing the integration time, the camera can be adapted to capture images with various

illumination conditions. For instance, during the summer with higher illumination conditions, the camera is set to a shorter integration time. In the winter or cloudy conditions, the integration time of the camera needs to increase.

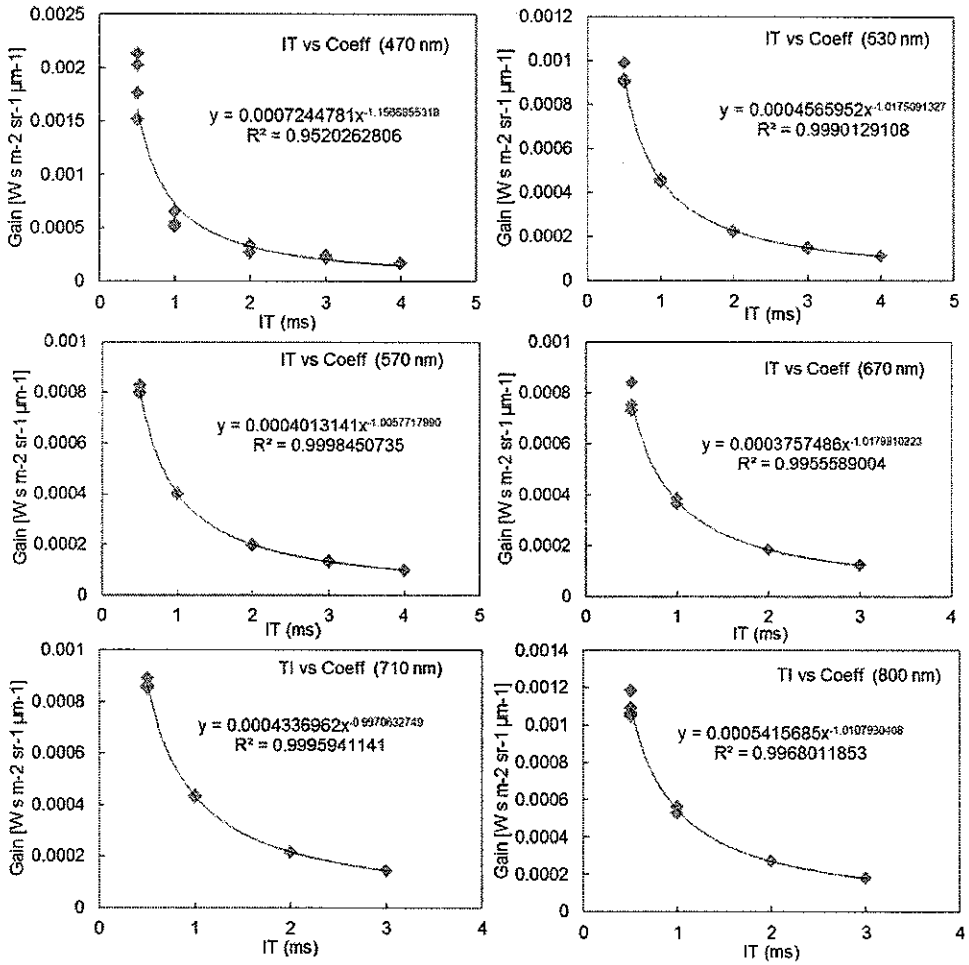

Figure 2. The gains for six bands of Tetra Mini-MCA6 with different integration time

3. Application

In January 2016, a test flight of a hexacopter with the Tetra Mini-MCA6 camera onboard was conducted at a DTU football pitch. The weather was sunny and the ground was covered with snow. But in order to get more heterogeneity of the surface, a small part of snow was remove and the grass underlying the snow could be seen (Figure 3). The UAV flight lasted 2 minutes and flying altitude is about 15.8 meter. 21 images were obtained from this test flight. We followed the workflow from Laliberte et al. (2011) to process these images with geometric and radiometric corrections. The geometric correction is based on the Agisoft Photoscan software and the radiometric correction is based

on the gain obtained at QuantaLab-IAS-CSIC by this STSM. The final orthophoto has 166m^2 coverage with the spatial resolution of 5.67mm. The "true color" of the orthophoto is shown in the Figure 3. With the gains in these six bands (Figure 2), the radiance of each band was also calculated as Figure 4. This is the first images of these six band radiance resulted by this STSM. In future, we will conduct more UAV-based remote sensing applications in Denmark and more results will be produced.

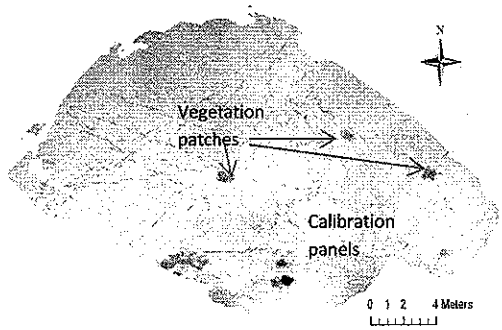

Figure 3. The orthophoto of the test region with snow cover (RGB color)

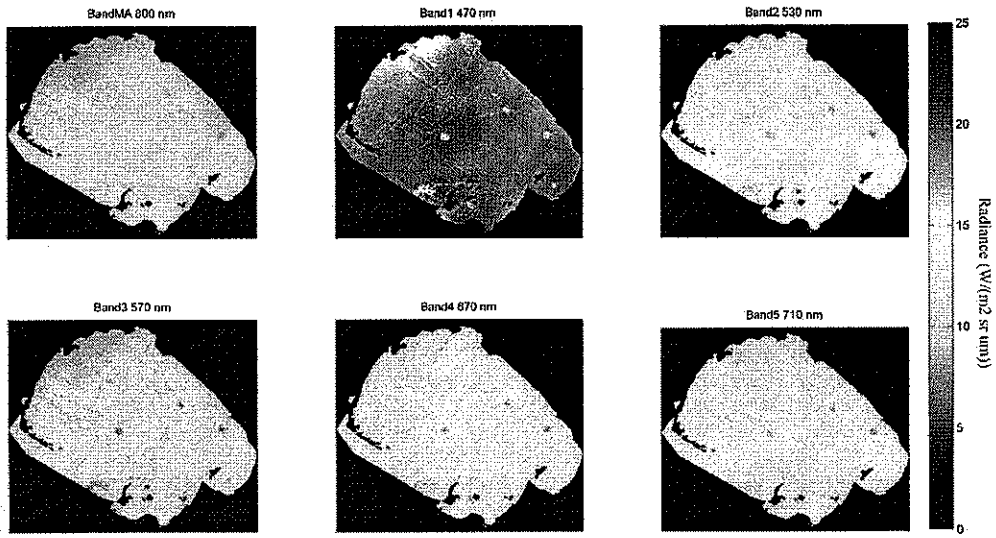

Figure 4. The radiance of calibrated images for each band

Future collaboration with the host institution

This STSM visiting reinforced the existing collaboration between DTU-Environment and QuantaLab-IAS-CSIC. In past, the researchers Dr. Pablo Zarco-Tejada and Dr. Monica Garcia (my supervisor) have been collaborating in thermal UAV research (Morillas et al., 2013; Morillas et al., 2009). The STSM extended the collaboration to the optical UAV remote sensing research. During this visit, I also

had chances to meet other members of QuantaLab-IAS-CSIC. Especially the technician Alberto Hornero Luque gave useful guidance and introductions on the radiometric calibration of the multispectral camera and shared useful experience on the UAV remote sensing research.

In the future, based on the calibrated multispectral camera, we will carry out more UAV-based remote sensing applications and researches in Denmark. We will also continue to collaborate with QuantaLab-IAS-CSIC on applying UAV techniques to improve our knowledge toward the mechanisms regulating the light use efficiency and water use efficiency of ecosystems, improving the hyperspatial land surface characterization, modeling and prediction, and to fill the scale gaps between in-situ observations and the coarse resolution satellite images.

Foreseen publications/articles resulting from STSM

Based on the outcome of this trip, we are able to use the calibrated multispectral camera to optically sample the underlying surface. Next step, we will move the UAV campaigns to the footprint of the eddy covariance flux tower. The orthophotos of vegetation indices and land surface temperature in the eddy covariance flux footprint will be produced. These data will further to be used to explore the heteorogeneity of the flux tower footprint and to improve the model simulation performance. Here, we foreseen following three papers resulting from this STSM.

1. Characterizing heterogeneity of underlying surface sampled by eddy covariance using a flux footprint model, Unmanned Aerial Vehicle (UAV) observations and a land surface model
2. Assimilation of Unmanned Aerial Vehicle (UAV) based vegetation indices for land surface modeling in a Danish heterogeneous agricultural landscape
3. Uncertainty quantification of simulated energy, carbon and water fluxes in a Danish willow field

Reference:

Ferrero, A., Campos, J., & Pons, A. (2006). Low-uncertainty absolute radiometric calibration of a CCD. Metrologia, 43, S17-S21.

Graham, R., Koh, A., Baltsavias, M., et al., (2004). Detectors and sensors. In: McGlone, J.C., Mikhail, E.M., Bethel, J. (Eds.) *Manual of Photogrammetry*, fifth ed. ASPRS, Bethesda, MA, pp. 505-580.

Laliberte, A. S., Goforth, M. A., Steele, C. M., & Rango, A. (2011). Multispectral remote sensing from unmanned aircraft: Image processing workflows and applications for rangeland environments. Remote Sensing, 3(11), 2529-2551.

Morillas, L., García, M., Zarco-Tejada, P., de Guevara M.L., Villagarcía, L., (2009). Obtaining vegetation conductance from spectral índices and surface temperatura to estimate evapotranspiration in semiarid vegetation (in Spanish). Congreso Internacional sobre Desertificación.

Morillas, L., Leuning, R., Villagarcia, L., Garcia, M., Serrano-Ortiz, P., & Domingo, F. (2013). Improving evapotranspiration estimates in Mediterranean drylands: The role of soil evaporation. Water Resources Research, 49(10), 6572-6586.

Shimano, N., Terai, K., & Hironaga, M. (2007). Recovery of spectral reflectances of objects being imaged by multispectral cameras. Journal of Optical Society of America, 24,3211-3219.